Rotational Invariance and Double Frustration in the Structures of Gold Clusters Growing around the F_s-Defected MgO (100) Surface

Giovanni Barcaro and Alessandro Fortunelli*

Molecular Modeling Laboratory, Istituto per i Processi Chimico-Fisici (IPCF) del C.N.R., via G. Moruzzi 1, 56124, Pisa, Italy

Received: July 17, 2006

The interaction of small gold clusters (Au_n, $n = 1-4$, 20) and a gold monolayer with the MgO (100) surface surrounding a neutral oxygen vacancy (F_s center) is investigated using density-functional (DF) calculations. It is found that the presence of the defect modifies the interaction of gold not only with the vacancy itself, but also with the oxygen and magnesium atoms around it by increasing both the adhesion energy and the equilibrium bond distances. This is at variance with the interaction of metal atoms with the regular MgO (100) surface or the F_s defect itself, in which an increase of the adhesion energy is associated with a shortening of the metal−surface distance. The resulting double frustration and cylindrical invariance of the metal−surface interaction cause small gold clusters growing around an F_s nucleation center to be highly fluxional in terms both of rotational freedom and of multiple competing structural motifs. Fragmentation energies of the gold clusters are also discussed, finding that the lowest-energy pathway corresponds to the detachment of a dimer.

1. Introduction

Metal nanoclusters have attracted much attention in recent years as a result of properties that are unique to the nanoscale domain.[1−4] In this context, gold nanoclusters play an important role: even though gold is the noblest of all metals,[5] a rich and often unexpected behavior shows up in gold nanoclusters,[6−8] ranging from selective low-temperature catalysis of industrially important reactions,[9−13] to peculiar optical[14,15] and electrical[16] properties, etc. In technological applications, stabilizing the metal clusters by coating with surfactants or through absorption on a substrate is an essential step to exploit the many fascinating properties of these materials. The (100) surface of the MgO oxide is a good candidate as an inert template for the cluster absorption.[17] The same inert characteristics of this surface, however, cause the growth of metal clusters to be strongly influenced by the presence of defects.[18,19] In this connection, the growth of gold clusters on the MgO (100) surface obtained via molecular-beam epitaxy (MBE) has been recently studied in great detail,[20,21] analyzing the dependence of the cluster density on the substrate temperature and the morphology of the resulting particles. From a theoretical point of view, several previous studies have confirmed that the interaction of gold with the regular MgO (100) surface is rather weak (less than 1 eV per atom).[22−24] The consequent need of nucleation centers to anchor the growth of metal deposition has promoted the study of extended and localized surface defects. In this context, the neutral oxygen vacancy (also known as F_s center) has been shown to be at the same time a common surface defect and able to act as a nucleation center for several transition metal species, including gold.[22−25] The strength of the Au atom/F_s center bond in fact is estimated to be greater than 2.5 eV,[22,23] thus providing a site at which nucleation can occur, as confirmed by a recent combined EPR and theoretical characterization of a single gold atom interacting with the regular and defected MgO (100) surface.[26] However, the evolution of the geometric structures of the metal clusters growing around the F_s center has been studied only for the smallest clusters and not systematically. The attention has mainly focused on the catalytic activity of small gold clusters rather than on the study of the growth process. For Au_n clusters in the range $n = 2-11$, some selected local minima structures atop neutral and charged defects (F_s and F_s^+ centers) have been considered in the light of the absorption properties of probe molecules (like CO or O_2);[13,27,28] this kind of study has been extended to consider optical properties of supported gold clusters[29] (with or without probe molecules absorbed atop them) or bigger metal aggregates absorbed on the regular (100) MgO surface.[30]

Small metal clusters have been the subject of intensive research in the past few years because they often exhibit peculiar low-energy configurations, different from those of larger aggregates.[31] The interaction with the substrate and its defects adds another degree of freedom and can induce further modifications into the cluster structure,[32,33] a topic of great interest both in view of the unusual properties that are often a consequence of these structural modifications and because the low-energy structures of small metal clusters can orient the subsequent growth. In fact, as the time-scale of the growth process is typically of the order of seconds or minutes (see, for example, ref 20), while the time-scale of the reorganization of small clusters (up to 50 atoms) can be estimated to be of the order of nanoseconds,[34] the metal clusters have the possibility to readjust their configurations to their low-energy structures.

Our aim in the present work is to understand the low-energy structures of small metal clusters growing around an F_s defect of the MgO (100) surface, and their connection with the basic energetics of the metal/defected-surface interaction. In a previous work,[22] we have presented a general investigation of the interaction of small coinage metal clusters and extended depositions with the regular and locally defected (100) MgO

* Corresponding author. Tel.: +39-050-3152247. E-mail: fortunelli@ipcf.cnr.it.

10.1021/jp064519e CCC: $33.50
Published on Web 09/20/2006

surface. In the present work, we report the results of systematic density-functional (DF) calculations focusing on the study of the interaction of small Au_n clusters ($n = 1-4$, 20) with a neutral oxygen vacancy defect. We show that this defect induces a long-range modification of the metal absorption characteristics in its surrounding and that this perturbation is responsible for the fluxionality of small clusters growing around the vacancy, possibly connected with the peculiar catalytic properties of small Au clusters[9,11,12,20,21] or the formation of clusters exhibiting different structural motifs.[21] Additionally, we calculate the fragmentation energies of clusters grown around the defect, finding that the lowest-energy pathway corresponds to the detachment of a dimer and involves energies that might be accessible in MBE experiments at high temperatures.

2. Computational Details

Density-functional (DF) calculations are performed using the PWscf (Plane-Wave Self-Consistent Field) computational code[35] employing ultrasoft pseudopotentials. The PBE exchange-correlation functional,[36] which is a gradient-corrected functional, is used. The kinetic energy cutoff for the selection of the plane-wave basis set is set at 40 Ry (1 Ry = 13.6 eV) for all of the calculations. A (4,4,1) *k*-point sampling of the Brillouin zone is chosen, and a Gaussian smearing procedure (with a smearing parameter of 0.002 Ry) is applied. The geometry optimizations are stopped when maximum force on atoms is less than 10^{-4} au. The distance between atoms in replicated cells is about 8−10 Å. The regular MgO (100) surface is modeled by a three-layer slab (as it is customary), each containing 18 (3×3 cell) or 32 (4×4 cell) Mg and O atoms fixed at the equilibrium lattice positions characterizing the MgO rock-salt structure (frozen at the experimental lattice constant of 4.208 Å). To produce a neutral F_s-defected surface, we remove one O atom from a surface layer, keeping the positions of all of the other atoms in the cell fixed. Larger (5×5) cells have been considered to check that the results on adhesion energies were not biased by the size of the cell. A general remark is here in order. DF theory using gradient-corrected (GGA) xc-functionals (such as PBE) makes the MgO system rather soft, as is proven by the fact that its lattice parameter at the DF-relaxed geometry is overestimated by about 2%. Hybrid xc-functionals would improve the description of the oxide, but they cannot be used here because of their bad description of the metal clusters (see, for example, ref 37), a common problem in the study of interfacial systems. Our experience then shows that, lacking clear experimental data to settle this problem, freezing the geometry of the oxide substrate at its experimental equilibrium configuration is the best choice so as not to let the DF/GGA approach overestimate the structural relaxation around the oxygen vacancy upon metal absorption. Anyway, we also checked that in the case of gold absorption the results were not qualitatively altered when allowing the substrate to relax.

3. Results and Discussion

We start with considering the absorption of a single Au atom on the regular and defected MgO (100) surface. We fix the Au position in the plane parallel to the oxide surface and optimize its distance from the surface. Figure 1 shows the resulting absorption topography, that is, the equilibrium distance and absorption energy as a function of the in-plane position, for both the regular and the defected surfaces.

A completely different energy and equilibrium distance landscape is immediately apparent in the two cases.

On the regular surface, one finds a rather flat potential energy surface, exhibiting minima in correspondence of the oxygen atoms, maxima on the magnesium atoms, and saddle points on the hollow sites, with a maximum adhesion energy of 0.91 eV and energy barriers of about 0.2 eV for the diffusion between neighboring oxygen sites. Correspondingly, the equilibrium height exhibits minima at 2.30 Å on the oxygen sites, maxima at 2.71 Å on the magnesium sites, and saddle points at 2.40 Å on the hollow sites. The in-plane distance between the energy minima corresponds to the MgO lattice parameter of about 2.97 Å: this value is larger than the typical Au−Au distances (the Au−Au distance in the bulk is 2.885 Å; smaller distances are normally found in Au nanoclusters), thus inducing a frustration (mismatch) in the metal growth on the MgO (100) surface.[38,39]

The presence of the F_s defect completely alters this situation,[32] with the resulting potential energy and equilibrium height surfaces exhibiting three major features: (I) the energy minimum in correspondence of the defect site is much deeper, with an adhesion energy of 3.07 eV; (II) a large basin of attraction is produced around the defect, with an adhesion energy of 1.62 eV on the magnesium atoms first-neighbors to the vacancy (to be compared to a value of 0.5 eV for the regular surface), extending its influence up to third neighbors, and exhibiting an approximate cylindrical symmetry, which is due to a strong perturbation of the electrostatic potential outside the surface with respect to the regular, nondefected system, which affects the polarization and thus the adhesion characteristics of the metal atom, as will be shown in detail in future work; and (III) there is a large difference between the equilibrium distance atop the defect (about 1.8 Å), strongly reduced with respect to the absorption onto the regular surface, and that atop the neighboring sites (2.65 Å on the magnesium and 2.59 Å on the oxygen sites first-neighbors to the vacancy, respectively), for which an increase in the absorption energy unexpectedly corresponds to an almost general increase in the equilibrium distance. The equilibrium distance then slowly relaxes to the values typical of the absorption on the regular surface as the Au atom gets farther from the defect. The topography of r_{min} as a function of the in-plane coordinates thus corresponds to a "crater" around the F_s center.

These three features determine the characteristics of the metal growth around the F_s defect.

First, due to the strong interaction of gold with the oxygen vacancy (I), this defect can act as an efficient trapping center for the nucleation of metal clusters.[22−25]

Second, the approximate cylindrical symmetry of E_{adh} around the defect site (II) ensures the metal clusters a considerable rotational freedom, by which the clusters can rotate on the surface keeping the atom atop the defect fixed, as the adhesion energy to the surface is essentially determined by the distance of the site with which the metal atom is interacting from the defect, rather than by its chemical identity.

The strong variation of r_{min} around the defect site (III) finally entails that the growth of metal clusters is frustrated not only "horizontally" with respect to the surface, due to the mismatch between MgO and Au lattice parameters, but also "vertically", due to the appreciable difference in the equilibrium height for the atom interacting directly with the F_s center and the neighboring atoms interacting with the surrounding sites, a feature which can be described as a "double frustration".

Point (I) is already known from previous work.[22−25] We will illustrate points (II) and (III) via examples of optimized structures of small Au clusters growing around the F_s center.

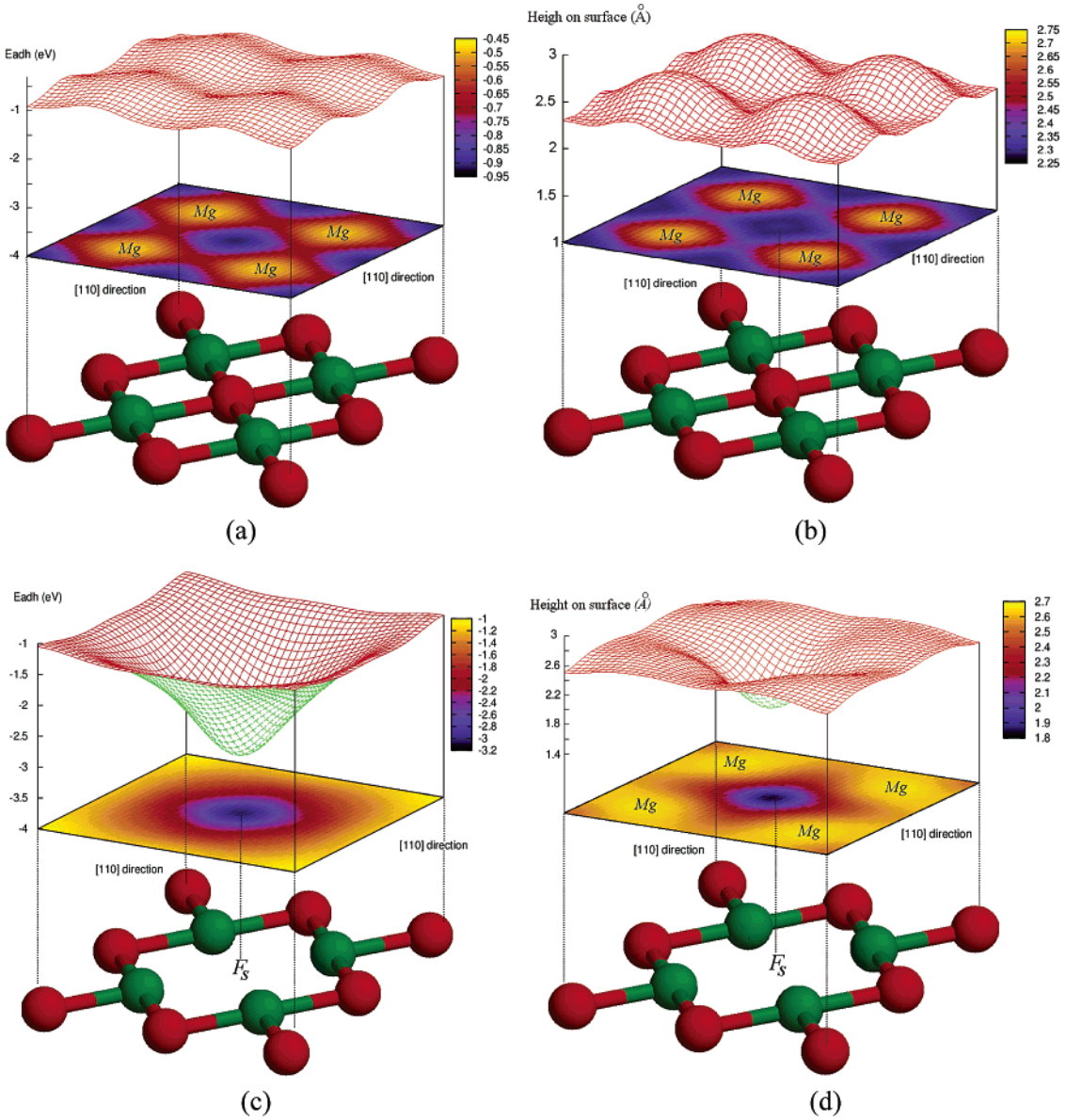

Figure 1. Topography of the absorption of an Au atom on the regular and defected MgO (100) surface: optimal adhesion energy (a) and equilibrium height (b) of a gold atom absorbed on the regular surface; optimal adhesion energy (c) and equilibrium height (d) of a gold atom absorbed on the F_s-defected surface.

The Au dimer minimum-energy structure is not shown, as it is known from previous work[22] to absorb on-top the F_s center in an upright position. In Figure 2, the Au_3 and Au_4 lowest-energy structures absorbed on the F_s-defected MgO (100) surface are shown, obtained through a search in which several (6−8) geometry optimizations starting from properly selected configurations have been conducted. In Table 1, the corresponding energies are reported. In addition, we also report in Figure 3 and Table 1 the structures and energy values for an Au_{20} cluster (a "magic" gold cluster recently characterized in the gas phase[40,41]) absorbed on the F_s center. This cluster has been chosen as an example of larger clusters and for its intrinsic interest: it is in fact a surface-only structure (no inner atoms), exhibiting a very large HOMO−LUMO gap of 1.77 eV, larger than that of C_{60},[40] an unusual stability and structure,[40,41] and peculiar optical[42,43] and catalytic[44] properties.

For each structure, we report in Table 1 four values of energy: (i) the adhesion energy (E_{adh}), calculated by subtracting the energy of the oxide surface and of the metal cluster, both frozen in their interacting configuration, from the value of the total energy of the system; (ii) the binding energy of the metal cluster (E_{met}), calculated by subtracting the energy of the isolated metal atoms from the total energy of the metal cluster in its interacting configuration; (iii) the metal cluster distortion energy (E_{dist}), which corresponds to the difference between the energy of the metal cluster in the configuration interacting with the surface, and the energy of the cluster in its lowest-energy gas-phase configuration; and (iv) the total energy (E_{tot}), which is the sum of the binding energy of the metal cluster and of the adhesion energy ($E_{tot} = E_{met} + E_{adh}$).

Let us start by illustrating the rotational freedom effect (II). The differences in total energy between configurations (b) and (c) of Au_3 or configurations (f) and (g) of Au_4 in Figure 2 (corresponding to the rotation of the trimer or tetramer around an axis perpendicular to the surface) are of the order of 0.02 eV. For such a "large" cluster as Au_{20}, one finds a similar situation, with an energy difference of 0.03 eV between configurations (a) and (b) in Figure 3, differing by a rotation around an axis perpendicular to the surface. For comparison, the energy differences among different Au_3 isomers on the

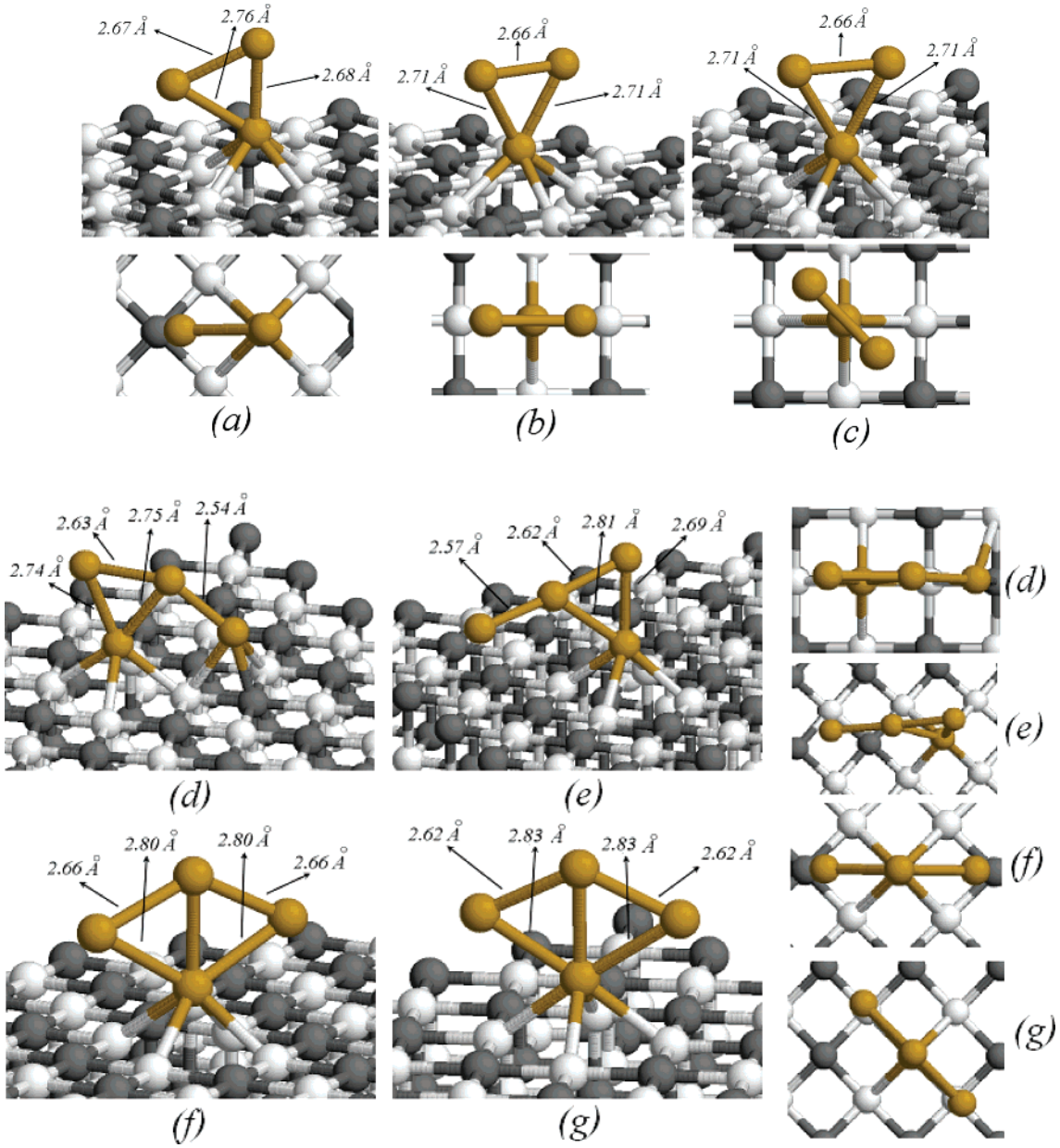

Figure 2. Lowest-energy local minima found for Au_3 and the Au_4 absorbed on an F_s defect from extensive DF searches. The corresponding energies are reported in Table 1.

TABLE 1: Energy Contributions Involved in the Absorption of Au_n (n = 3, 4, 20) Clusters on the F_s-Defected Oxide Surface[a]

	configuration	E_{adh} (eV)	E_{met} (eV)	E_{dist} (eV)	E_{tot} (eV)
Au_3	(a)	3.95	3.57	0.02	7.52
	(b)	3.96	3.56	0.03	7.52
	(c)	3.93	3.57	0.02	7.50
Au_4	(d)	4.57	5.80	0.46	10.37
	(e)	4.25	6.12	0.15	10.37
	(f)	4.04	6.20	0.06	10.24
	(g)	4.13	6.09	0.17	10.22
Au_{20}	(a)	4.33	46.25	0.72	50.58
	(b)	4.14	46.41	0.56	50.55

[a] The total energy of absorption (E_{tot}) is the sum of the metal bond contribution (E_{met}) and of the adhesion contribution (E_{adh}). The bigger is the value of E_{tot}, the more stable is the corresponding configuration. The metal distortion contribution (E_{dist}) is also reported.

regular surface are in the range 0.04−0.13 eV.[22] Small Au clusters absorbed on an oxygen vacancy are thus "rotationally fluxional" with respect to the absorption onto the surface.

The results in Figure 2 and Table 1 also illustrate the effects of the double frustration (III). A typical consequence is the fact that one finds configurations that are structurally different, but nearly isoenergetic; that is, one finds a competition between configurations with a reduced adhesion energy and a stronger metallic bond versus "doubly frustrated" configurations in which the metal cluster deforms appreciably with respect to the gas-phase situation to be in registry with the equilibrium energy and height topography shown in Figure 1 and thus increase its adhesion energy. Examples of this competition are structures (a) versus (b) of Au_3 and structures (d) versus (f) of Au_4. In the structures with a larger adhesion energy, the effect of the additional frustration produced by the F_s center is apparent: one finds an elongation of the metal−metal bond length between the atom atop the vacancy and its neighbors, as in structures (a) of Au_3, (d) of Au_4, and (a) of Au_{20}. These strained metal−metal bonds reflect in the larger values of E_{dist}. Alternatively, the cluster can essentially maintain its gas-phase equilibrium structure and adhere to the surface mainly through the atom

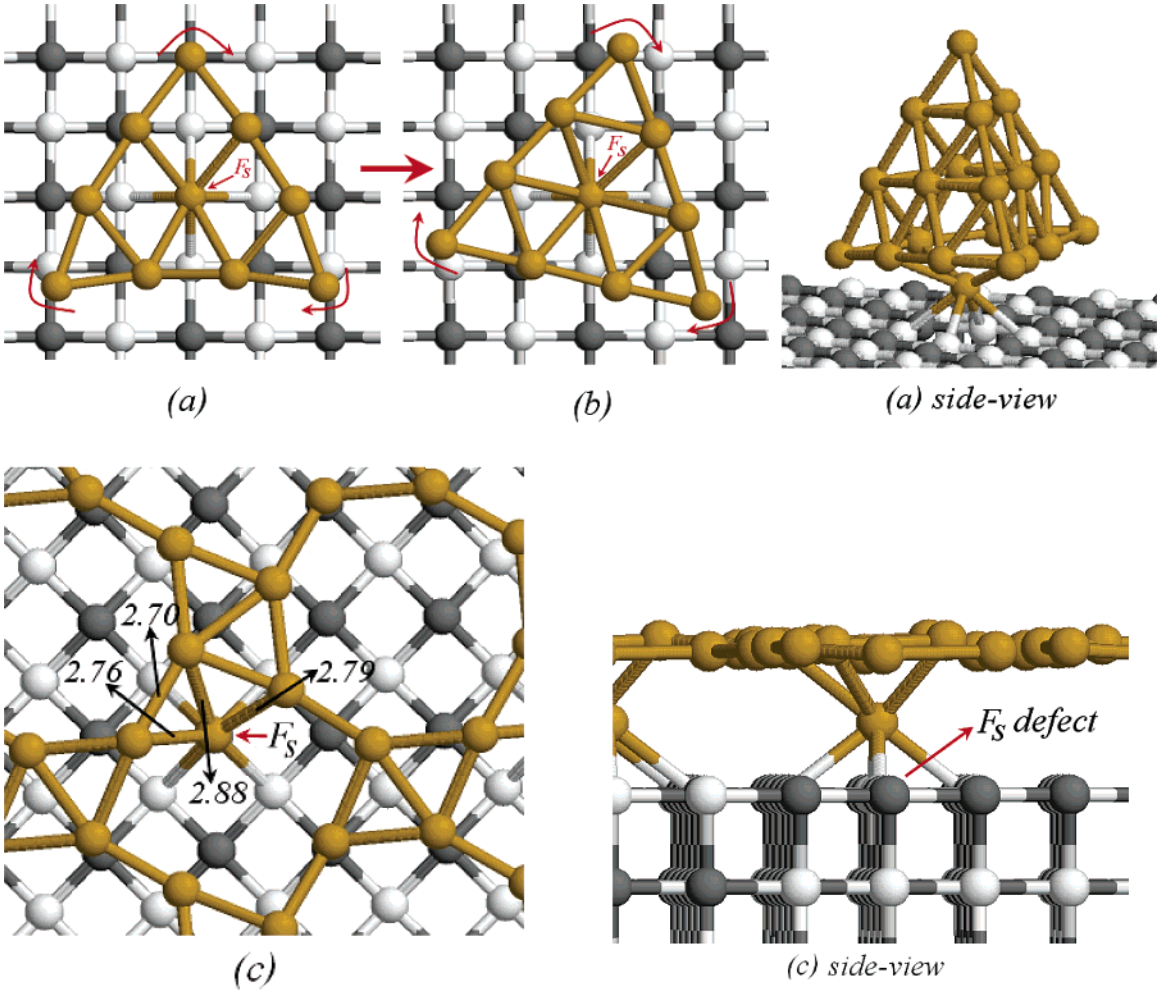

Figure 3. Low-energy configurations for Au_{20} (a,b) and a gold monolayer (c) are displayed: (b) is obtained from (a) through a rotation of about 30° around an axis perpendicular to the surface; on the right, a side-view of the (a) configuration is displayed to highlight the strong deformation of the basal fcc (111) face; (c) Au monolayer reconstruction around the F_s vacancy in the 3 × 3 cell; the elongated metal bond lengths shown are due to the frustration induced by the oxide defect.

directly atop the vacancy, as in structures (b) of Au_3 or (f) of Au_4. It is interesting to observe from Figure 3 that absorbed Au_{20} substantially maintains its "magic" tetrahedral structure, with the notable exception of the atom at the center of the basal fcc (111) face, which protrudes out and elongates its metal−metal bonds to better interact with the oxygen vacancy. One can also note that, despite the very similar values of the total absorption energy, the Au_{20} cluster is more deformed in structure (a), see especially the atoms at two basal apexes, with respect to structure (b). The metal distortion energy is, however, not large enough to overcome the extra stability associated with the electronic shell closure, cage-like and local-fcc-pattern effects,[41] so that the tetrahedral structure is a good candidate as the global minimum of Au_{20} absorbed on the MgO (100) F_s defect. If confirmed, this implies that tetrahedral Au_{20} absorbed on MgO (100) may possess peculiar optical and catalytic properties.[42−44] A further illustration of the effects of double frustration is given in Figure 3c, in which the configuration resulting from the geometry optimization of a gold monolayer in a 3 × 3 cell is shown: one finds a peculiar clusterization induced by the presence of the F_s defect. In particular, the Au atom atop the vacancy gets much closer to the surface (1.62 Å) with respect to the neighboring atoms (distances in the range 3.2−3.5 Å), as it is apparent from the side-view of Figure 3c, and this is the origin of the clusterization effect. We note in passing that this is an example of 2D structures, which have been advocated for gold deposition on oxide substrates.[12] To summarize point (III), we can say that the peculiar topography of r_{min} around the vacancy gives rise to a different form of cluster fluxionality, in which the cluster's energy landscape is populated with nearly isoenergetic, but qualitatively diverse structural motifs. A precise understanding of metal clusters' fluxionality is important as it can have a substantial influence, for example, on the clusters' catalytic properties,[13,20,21] or explain the experimentally observed formation of metal clusters exhibiting different structural motifs.[20,21]

In passing, we note that we have not discussed the configurations derived from our local energy minimizations lying at high energies. Kinetic trapping effects involving high-energy local minima could occur if the dynamics of the growth process is much faster than that of the cluster reorganization. However, the experimental flow (or deposition) rate is usually kept small to increase the reproducibility of the results, so the time-scale of the growth process is typically of the order of seconds or minutes (see, for example, ref 20), much larger than the time-scale of the reorganization of small clusters (of the order of nanoseconds[34]). Kinetic effects involving high-energy minima are therefore not likely in the usual experimental conditions.

To conclude the analysis of the results reported in Table 1, we consider the energetics of processes in which a metal cluster absorbed on an F_s center dissociates into two smaller clusters: one still absorbed on the defect, and the other one on the regular

TABLE 2: Energy Differences Corresponding to Metal Cluster Dissociation Processes[a]

process	energy difference (eV)
$Au_2(d) \rightarrow Au(d) + Au(r)$	1.87
$Au_3(d) \rightarrow Au_2(d) + Au(r)$	0.75
$Au_3(d) \rightarrow Au(d) + Au_2(r)$	0.70
$Au_4(d) \rightarrow Au_3(d) + Au(r)$	1.96
$Au_4(d) \rightarrow Au_2(d) + Au_2(r)$	0.79
$Au_4(d) \rightarrow Au(d) + Au_3(r)$	2.07

[a] $Au_n(d)$ and $Au_n(r)$ represent clusters lying on the F_s-defected or the regular surface, respectively. The energies used to calculate these differences are the total energies reported in Table 1 for the clusters absorbed on the defect. The total absorption energy of a dimer on the defect is 5.85 eV. The total cluster absorption energies on the regular surface are: Au_1, 0.91 eV; Au_2, 3.74 eV; Au_3, 5.30 eV.

surface. These processes can be important[33,45] for understanding detrapping and thus Ostwald ripening of small clusters by larger ones observed in MBE experiments at sufficiently high temperatures.[20,21] In Table 2, we report the energy differences corresponding to several fragmentation processes of Au_n clusters. $Au_n(d)$ and $Au_n(r)$ represent clusters lying on the defect or the regular surface, respectively. The most interesting finding from these results is that dissociation of a dimer (Au_2) fragment as a rule requires substantially less energy than that of a single atom or a trimer. This is due to two reasons: (a) an Au_2 dimer both on the regular surface or atop an oxygen vacancy is stabilized by the "metal-on-top" effect,[22] that is, by an increase in the metal−surface adhesion due to the presence of metal atoms above those directly interacting with the surface; and (b) the double frustration around the defect strains the Au−Au distance between the Au atom atop the defect and those atop neighboring sites and destabilizes the Au_3 and Au_4 clusters with respect to a single atom or a dimer on the oxygen vacancy, whose optimal geometry is in an upright position and does not involve the interaction of metal atoms with sites surrounding the vacancy. As a consequence, we see from Table 2 that extraction of an $Au_2(r)$ fragment from $Au_3(d)$ or $Au_4(d)$ requires 0.7/0.8 eV. This energy difference is not large as compared to k_BT in MBE experiments,[20,21] which suggests that fragmentation processes of small clusters may be active and should be taken into account in the growth and sintering of Au clusters at sufficiently high temperatures.[33,45]

4. Conclusions

We find that the presence of a neutral oxygen vacancy (F_s center) appreciably modifies the potential energy landscape of a gold atom moving in its surrounding, and that this has important consequences on the growth of small gold clusters atop the defect site. An accurate sampling of the single-atom absorption topography highlights that not only the interaction of the gold atom directly atop on the defect is strongly increased, and its equilibrium distance from the surface decreased, but the absorption over a larger region extending up to third- and fourth-neighbor sites is appreciably altered. Unexpectedly, (a) similar interaction energies are found for the neighboring oxygen and magnesium sites, which therefore lose their chemical identity, and (b) both the absorption energies and the equilibrium heights are increased with respect to the regular surface. The latter effect induces what can be described as a "double frustration", in the sense that it adds to the usual frustration due to the mismatch between oxide and bulk metal lattice parameters. All of this produces a rotational and structural fluxionality of the gold clusters absorbed on the F_s defect, by which (a) the clusters can almost freely rotate around an axis perpendicular to the surface, leaving the atom directly interacting with the defect site fixed; and (b) one finds a competition between metal cluster configurations with a reduced absorption energy, but a small distortion with respect to the gas-phase structure and thus a stronger metallic bond, and configurations in which the metal−metal distances between the atom atop the defect and its nearest neighbors are elongated (double frustration), but the overall configuration is stabilized by larger adhesion energies. This is explicitly shown for the Au_3 and Au_4 lowest-energy structures, and for the tetrahedral Au_{20} and a gold monolayer absorbed on an oxygen vacancy. This fluxionality can have a substantial influence, for example, on the clusters' catalytic properties,[13,20,21] or explain the experimentally observed formation of metal clusters exhibiting different structural motifs.[20,21]

Additionally, we also calculate cluster fragmentation energies, corresponding to partial detrapping from the defect site, and find that the extraction of a gold dimer involves energies around 0.7/0.8 eV, and might thus be active[45] in MBE experiments at sufficiently high temperatures[20] (Ostwald ripening).

Finally, we stress that this behavior is not peculiar of gold, but is qualitatively quite general, and has been verified by us also for other metals (e.g., Ag) growing around an MgO (100) oxygen vacancy, as will be reported in future work.

Acknowledgment. We acknowledge financial support from the Italian CNR for the project "(Supra-)Self-Assemblies of Transition Metal Nanoclusters" within the framework of the ESF EUROCORES SONS, and from the European Community Sixth Framework Program for the STREP project "Growth and Supra-Organization of Transition and Noble Metal Nanoclusters" (contract no. NMP4-CT-2004-001594).

References and Notes

(1) de Heer, W. A. *Rev. Mod. Phys*. **1993**, *65*, 611.
(2) *Chemisorption and Reactivity on Supported Clusters and Thin Films*; NATO Advanced Study Institute, Series E: Physics; Lambert, R. M., Pacchioni, G., Eds.; Kluwer: Dordrecht, 1997; Vol. 331.
(3) Klabunde, K. J. *Nanoscale Materials in Chemistry*; Wiley: New York, 2001.
(4) *Progress in Experimental and Theoretical Studies of Clusters*; Kondow, T., Mafuné, F., Eds.; World Scientific: New York, 2003.
(5) Hammer, B.; Norskov, J. K. *Nature* **1995**, *376*, 238.
(6) Schwerdtfeger, P. *Angew. Chem., Int. Ed.* **2003**, *42*, 1892.
(7) Daniel, M.-C.; Astruc, D. *Chem. Rev.* **2004**, *104*, 293.
(8) Pyykkö, P. *Angew. Chem., Int. Ed.* **2004**, *43*, 4412.
(9) Hutchings, G. J.; Haruta, M. *Appl. Catal., A* **2005**, *291*, 2.
(10) Remediakis, N.; Lopez, N.; Norskov, J. K. *Appl. Catal., A* **2005**, *291*, 13.
(11) Haruta, M. *Chem. Rec.* **2003**, *3*, 75.
(12) Chen, M. S.; Goodman, D. W. *Science* **2004**, *306*, 252.
(13) Häkkinen, H.; Abbet, S.; Sanchez, A.; Heiz, U.; Landman, U. *Angew. Chem., Int. Ed*. **2003**, *42*, 1297.
(14) Zheng, J.; Dickson, R. M. *J. Am. Chem. Soc*. **2002**, *124*, 13982.
(15) Brongersma, M. L. *Nat. Mater*. **2003**, *2*, 296.
(16) Chen, S.; Ingram, R. S.; Hostetler, M. J.; Pietron, J. J.; Murray, R. W.; Schaaff, T. G.; Khoury, J. T.; Alvarez, M. M.; Whetten, R. L. *Science* **1998**, *280*, 2098.
(17) Lee, Y. C.; Tong, P.; Montano, P. A. *Surf. Sci*. **1987**, *181*, 559.
(18) He, J.-W.; Moller, P. J. *Surf. Sci.* **1987**, *180*, 411.
(19) Haas, G.; Menck, A.; Brune, H.; Barth, J. V.; Venables, J. A.; Kern, K. *Phys. Rev. B* **2000**, *61*, 11105.
(20) Horup-Hansen, K.; Ferrero, S.; Henry, C. R. *Appl. Surf. Sci*. **2004**, *226*, 167.
(21) Meerson, O.; Sitja, G.; Henry, C. R. *Eur. Phys. J. D* **2005**, *34*, 119.
(22) Barcaro, G.; Fortunelli, A. *J. Chem. Theory Comput.* **2005**, *1*, 1972.
(23) Del Vitto, A.; Pacchioni, G.; Delbecq, F.; Sautet, P. *J. Phys. Chem. B* **2005**, *109*, 8040. The numerical differences of the absorption energies with respect to ref 22 are due to a different description of the oxide structural properties.
(24) Yudanov, I.; Pacchioni, G.; Neyman, K.; Rösch, N. *J. Phys. Chem. B* **1997**, *101*, 2786.

(25) Matveev, A. V.; Neyman, K.; Yudanov, I.; Rösch, N. *Surf. Sci.* **1999**, *426*, 123.
(26) Yulikov, M.; Sterrer, M.; Heyde, M.; Rust, H.-P.; Risse, T.; Freund, H.-J.; Pacchioni, G.; Scagnelli, A. *Phys. Rev. Lett.* **2006**, *96*, 146804.
(27) Sanchez, A.; Abbet, S.; Heiz, U.; Schneider, W.-D.; Häkkinen, H.; Barnett, R. N.; Landman, U. *J. Phys. Chem. A* **1999**, *103*, 9573.
(28) Molina, L. M.; Hammer, B. *J. Chem. Phys.* **2005**, *123*, 161104.
(29) Walter, M.; Häkkinen, H. *Phys. Rev. B* **2005**, *72*, 205440.
(30) Molina, L. M.; Hammer, B. *Phys. Rev. B* **2004**, *69*, 155424.
(31) Baletto, F.; Ferrando, R. *Rev. Mod. Phys.* **2005**, *77*, 371.
(32) Moseler, M.; Hakkinen, H.; Landman, U. *Phys. Rev. Lett.* **2002**, *89*, 176103.
(33) Giordano, L.; Di Valentin, C.; Goniakowski, J.; Pacchioni, G. *Phys Rev. Lett.* **2004**, *92*, 096105.
(34) Baletto, F.; Mottet, C.; Ferrando, R. *Phys. Rev. Lett.* **2000**, *84*, 5544.
(35) Baroni, S.; Del Corso, A.; de Gironcoli, S.; Giannozzi, P., http://www.pwscf.org.
(36) Perdew, J. P.; Burke, K.; Ernzerhof, M. *Phys. Rev. Lett*. **1996**, *77*, 3865.
(37) Aprà, E.; Fortunelli, A. *J. Mol. Struct. (THEOCHEM)* **2000**, *501*−*502*, 251.
(38) Vervisch, W.; Mottet, C.; Goniakovski, J. *Phys. Rev. B* **2002**, *65*, 245411.
(39) Leroy, F.; Renaud, G.; Letoublon, A.; Lazzari, R.; Mottet, C.; Goniakowski, J. *Phys. Rev. Lett.* **2005**, *95*, 185501.
(40) Jun, L.; Li, X.; Zhai, H. J.; Wang, L. S. *Science* **2003**, *299*, 864.
(41) Aprà, E.; Ferrando, R.; Fortunelli, A. *Phys. Rev. B* **2006**, *73*, 205414.
(42) Wu, K.; Li, J.; Lin, C. *Chem. Phys. Lett*. **2004**, *388*, 353.
(43) Xie, R.-H.; Bryant, G. W.; Zhao, J.; Kar, T.; Smith, V. H. *Phys. Rev. B* **2005**, *71*, 125422.
(44) Molina, L. M.; Hammer, B. *J. Catal*. **2005**, *233*, 399.
(45) Xu, L.; Henkelman, G.; Campbell, C. T.; Jonsson, H. *Phys Rev. Lett.* **2005**, *95*, 146103.